Nucleic Acids Research, 1996, Vol. 24, No. 23 **4759–4767**

# Real-time imaging of the reorientation mechanisms of YOYO-labelled DNA molecules during 90° and 120° pulsed field gel electrophoresis

**Sergio Gurrieri[1,2,3,*], Steven B. Smith[3], K. Sam Wells[4], Iain D. Johnson[4] and Carlos Bustamante[3,5]**

[1]Dipartimento di Scienze Chimiche, Universita' di Cantania, Viale A. Doria 6, 95125 Catania, Italy, [2]Instituto per lo Sudio delle Sostanze Naturali di Interesse Alimentare e Chimico-Farmaceutico, CNR, Via del Santuario 110, 95028 Valverde (CT), Italy, [3]Department of Chemistry and Institute of Molecular Biology, University of Oregon, Eugene, OR 97403, USA, [4]Molecular Probes, Inc., 4849 Pitchford Avenue, Eugene, OR 97402, USA and [5]Howard Hughes Medical Institute, University of Oregon, Eugene, OR 97403, USA

Received August 5, 1996; Revised and Accepted October 10, 1996

## ABSTRACT

**Pulsed field gel electrophoresis (PFGE) techniques have been developed to overcome the limitations of conventional electrophoresis and to increase the separation to DNA chromosomes of few megabase pairs in size. Despite of the large success of these techniques, the various separation protocols employed for PFGE experiments have been determined empirically. However, a deep understanding of the molecular mechanisms of motion responsible for DNA separation becomes necessary for the rational optimization of these techniques. This paper shows the first clear observations of individual molecules of DNA during the reorientation process in 90° PFGE and 120° PFGE. Real-time visualization of the DNA dynamics during PFGE was possible with the use of an epi-illumination fluorescence microscope specifically equipped to run these experiments and by staining the DNA with YOYO-1 (1,1′-(4,4,7,7-tetramethyl-4,7-diazaundecamethylene)-bis-4-[3-methyl-2,3-dihydro-(benzo-1,3-oxazole)-2-methyl-idene]-quinolinium tetraiodide). This dye forms a very stable, highly fluorescent complex with double-stranded DNA and dramatically improves the quality of the DNA images. The results of computer simulations used to reproduce the molecular mechanisms of motion as well as the DNA separation features are also discussed.**

## INTRODUCTION

Conventional (steady-field) agarose gel electrophoresis is the most widely used method for separating small DNA molecules by size. However, for DNA chains approaching ~10–20 kb the electrophoretic mobility μ becomes increasingly independent of molecular size (1–2). The DNA size at which μ becomes independent of the length of the nucleic acid depends strongly on the electrophoretic conditions employed and, in particular, on the electric field strength and the agarose concentration (3–4).

To overcome this limitation, a whole series of pulsed field gel electrophoresis (PFGE) techniques have been developed (5–17). In typical PFGE experiments, DNA molecules are present in an ordinary agarose gel matrix in conventional low-ionic strength buffers. An electric field of ~10 V/cm, but sometimes considerably lower, is applied alternately in two directions. Pulse times can range from less than a second to several minutes or more, depending on molecular size. The various techniques differ mainly in the configuration of the electrodes around the gel to create the two alternating electric fields and in the angle between these fields. Since most of these techniques are characterized by similar separation features, in this paper we will refer to as 90° and 120° PFGE, simply indicating the angle between the electric fields, independently on the way these fields are generated. Using PFGE, separation of DNA molecules as long as ~5 Mb pairs can be achieved (18).

However, even if these techniques turned out to be so successful, the various separation protocols employed for PFGE experiments have been determined empirically, while descriptions of the molecular mechanisms of motion responsible for DNA separation have lagged behind (19–26). Since the discovery of the original PFGE methods, several mechanisms of DNA reorientation have been proposed in order to provide a physical explanation of the success of these techniques (27–29). In fact, in order to migrate through the gel matrix, the DNA molecules have to change their direction of motion in response to the changing electric field, and size separation must depend on the way the molecules reorient when the electric field changes direction. Most of these reorientation mechanisms predict a linear dependence of reorientation time on DNA size. As long as the reorientation time is shorter than the pulse time, the mobility becomes linearly dependent on size. In fact, according to these ideas (29), the DNA mobility should depend only on the fraction of each pulse

*To whom correspondence should be addressed. Tel: +39 95 330 037; Fax: +39 95 580 138; Email: sgurrieri@dipchi.unict.it

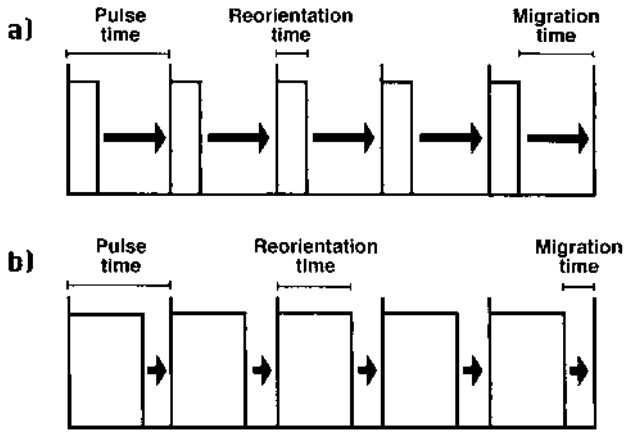


**Figure 1.** Dependence of PFGE mobility on molecular reorientation time. The two panels show the expected results for two DNA molecules of different sizes. DNA mobility depends on the fraction of each pulse remaining for net migration after reorientation has been completed. The arrows show the amount of forward motion occurring in each pulse cycle. (**a**) Short molecules have short reorientation times and spend most of the pulse time migrating through the gel before the field is switched in direction. (**b**) Instead, long DNA molecules need a long time for the reorientation process, therefore using only a short fraction of the pulse time for net migration. (Modified from ref. 29).

remaining for net migration. Short molecules will reorient very rapidly in the direction of the new field and will spend a good fraction of the pulse time migrating through the gel before the electric field is switched again (Fig. 1a). On the contrary, long DNA molecules will spend most of the pulse time for the reorientation process, thus having only a short time available for actual migration (Fig.1b). As will be shown later, this idea is much too simple and only partially correct because other features of the reorientation mechanisms become more important in determining size separation.

This paper shows the first clear visualization of individual DNA molecules of intermediate-size (50 kb–1 Mb) during the reorientation process in 90° PFGE and 120° PFGE. Real-time imaging experiments were possible by using custom made electrophoresis microchambers together with an epi-illumination fluorescence microscope equipped with a high gain image intensifier and a high sensitivity video camera, designed specifically for critical low-light imaging. Also, a dramatic improvement in the quality of the DNA images was accomplished by labeling the DNA with YOYO-1 (30–35). In fact, YOYO-1 forms a very stable, highly fluorescent complex with double-stranded DNA and undergoes ~500-fold fluorescence enhancement upon binding. Moreover, the high affinity of YOYO-1 for DNA makes it possible to use very low DNA and dye concentrations such that only one or few bright molecules can be seen in the field of view of the microscope against a dark and homogeneous background. Finally, in order to characterize, unambigously, the molecular mechanisms of DNA motion and the basis for separation in PFGE, computer simulations (24,36–37) were used in combination with the fluorescence microscopy observations.

## MATERIALS AND METHODS

### Spectroscopic and binding affinity measurements

Measurements were performed using an IBM instruments 9420 spectrophotometer. Polystyrene cuvettes were employed to minimize surface adsorption of the polycationic YOYO-1. To determine the molar extinction coefficients ($\varepsilon_{max}$) for the DNA-bound dyes, 100 µl of a concentrated Calf thymus DNA (Sigma) stock solution ($5 \times 10^{-3}$ moles of bp/l) were added to 2.5 ml of a $4 \times 10^{-6}$ M dye solution in 10 mM Tris–HCl, pH 7.4 to yield a molar ratio of ~50 DNA bp per dye molecule. The DNA–dye complex was allowed to equilibrate for at least 90 min. The change in the maximum absorbance relative to the aqueous free dye, after correction for the dilution due to DNA addition was converted to give $\varepsilon_{max}$ for the complex.

Either a PTI Alphascan or an SLM-500C spectrofluorometer were employed to record fluorescence measurements. Solutions typically contained $4 \times 10^{-7}$ M dye in 10 mM Tris–HCl, 50 mM NaCl, 1 mM EDTA, pH 7.4 and $2 \times 10^{-5}$ moles of bp/l Calf thymus DNA, equilibrated as above. Fluorescence quantum yields ($\phi_F$) for these samples were determined relative to fluorescein in 0.1 M NaOH (38). Appropriately oriented polarizers were used to eliminate the possible effects of non-isotropic fluorescence emission from the DNA–dye complexes. The fluorescence enhancement on DNA binding, Ψ, (the ratio of the fluorescence quantum yield for a dye molecule bound to DNA, $\phi_{bound}$, over the fluorescence quantum yield of a dye molecule free in solution, $\phi_{free}$) was determined by measuring and integrating the respective fluorescence emission spectra with the excitation at the isosbestic point between the corresponding absorption spectra. Careful subtraction of background signals measured using a dye-free blank was necessary for accurate quantitation of the very weak emission of YOYO-1 free in solution.

The binding affinities of ethidium bromide and acridine orange were determined by measuring the fluorescence enhancement (ΔF), at a fixed low concentration of dye, as function of DNA concentration [DNA] (expressed in moles of bp/l). The x-intercept of a linear plot of 1/ΔF versus 1/[DNA] is equal to the binding affinity, $K_a$. Double-stranded Calf thymus DNA was titrated against a fixed concentration of fluorescent dye ([EB] = [AO] = $10^{-7}$ M) in phosphate buffer (10 mM $Na_2PO_4$, pH 7.0, containing 1 mM EDTA and 100 mM NaCl). The binding affinity for YOYO-1 was obtained from reference (39).

### Preparation of samples for imaging experiments

All the samples used for imaging were prepared using T2 phage genomic DNA (164 kb) purchased from Sigma Chemical Co. A stock solution of T2 phage DNA ($1.95 \times 10^{-4}$ moles of bp/l = 125 µg/ml) was prepared by dissolving the lyophilized DNA in 2 ml of distilled water and was stored refrigerated at 5°C. In the preparation of the solutions for our experiments, micro-pipettes with cut tips were used to minimize DNA breakage. All dyes—YOYO-1, ethidium bromide and acridine orange—were provided by Molecular Probes, Inc. Their stock and working solutions and also the DNA–dye solutions were stored in plastic vials at 5°C in the dark. It was found that YOYO-1 partitions from aqueous solution, even when complexed with DNA, onto glass surfaces. Aqueous solutions of YOYO-1 appear to be indefinitely stable when kept in plastic containers. Storage in glass is practical for DMSO solutions.

Stock solutions of YOYO-1 ($1.0 \times 10^{-3}$ M) were prepared by dissolving solid YOYO-1 in dimethyl-sulphoxide (DMSO). The concentration was obtained by measuring the absorbance in methanol using $\varepsilon_{481}$= 125 800. Working solutions of YOYO-1 ($1 \times 10^{-5}$ M) were prepared by dilution in 0.5× Tris–borate–EDTA

(TBE) buffer (45 mM Tris, 45 mM Borate, 1 mM EDTA, pH 8.2). Staining of T2 DNA was accomplished by incubating overnight T2 DNA ($5\times10^{-6}$ moles of bp/l) and YOYO-1 ($1\times10^{-6}$ M) at a DNA bp/YOYO-1 ratio of 5:1. This solution was then diluted 1000-fold in 0.5× TBE containing 2% (v/v) β-ME (β-mercaptoethanol). The final concentrations were: $5\times10^{-9}$ moles of bp/l T2 DNA, $1\times10^{-9}$ M YOYO-1, 2% (v/v) β-ME. Eight µl of this final solution were put on a microscope glass slide and a 22 × 22 mm coverslip was placed on top and sealed with fingernail polish or molten candle wax. For the electrophoresis experiments a suspension of 1% (w/v) ME SeaKem agarose gel (FMC Bioproducts) in 0.5× TBE buffer (45 mM Tris, 45 mM borate, 1 mM EDTA) was prepared. After 5 min this suspension was gently boiled for 5 min and then cooled down to 50°C. Distilled water was used to restore the water lost by evaporation. β-ME was added to a concentration of 2%. The 5:1 DNA/YOYO-1 concentrated solution ($5\times10^{-6}$ moles of bp/l T2 DNA, $1\times10^{-6}$ M YOYO-1) was diluted 1000-fold in the molten gel. The final concentrations were: 1% agarose, $5\times10^{-9}$ moles of bp/l T2 DNA, $1\times10^{-9}$ M YOYO-1, 2% β-ME (v/v). Ten µl of this mixture were put on top of a microscope slide already equipped with electrodes, and pre-heated at 50°C. A 22 × 22 mm coverslip was placed on top and sealed at the four corners with fingernail polish. The gel was allowed to solidify for 10 min at room temperature. The electrical connection was completed by dropping molten gel over the electrodes and 0.5× TBE buffer was only occasionally added to keep it wet.

In order to overcome the inevitable photosensitivity of the DNA–YOYO-1 complex under sustained high illumination conditions (40), particular care was taken to deoxygenate all the solutions and assembling the microscope slides under nitrogen atmosphere in a custom made glove box. Oxygen was removed from the samples by carefully bubbling nitrogen through all the DNA samples, as well as through the molten agarose gel (kept at a constant temperature of 50°C) for ~10 min. Also, particular care was taken to flow nitrogen onto the electrophoresis micro-chamber and coverslips during the assembling process. Using such a procedure, in combination with the use of β-ME, it was possible to minimize strand breaking and to extend the lifetime of the molecules to several minutes. When DNA brightness was not critical, neutral density filters were employed to reduce the excitation intensity and, therefore, to increase further the durability of the experiments.

Stock solutions of ethidium bromide ($1.3\times10^{-2}$ M) were prepared by dissolving solid ethidium bromide in distilled water. The concentration was obtained by measuring the absorbance in water using $\varepsilon_{481}$ = 5448. Staining of T2 DNA was accomplished by incubating overnight T2 DNA ($1.6\times10^{-6}$ moles of bp/l) and ethidium bromide ($1.3\times10^{-5}$ M). This solution was then diluted 10-fold in 0.5× TBE containing 2% (v/v) β-ME. The final concentrations were: $1.6\times10^{-7}$ moles of bp/l T2 DNA, $1.3\times10^{-6}$ M EtBr, 2% (v/v) β-ME. Eight µl of this solution were used to prepare the microscope slides as described before.

Stock solutions of acridine orange ($1.1\times10^{-3}$ M) were prepared by dissolving solid acridine orange in distilled water. The AO concentration was determined by its absorbance in water using $\varepsilon_{493}$ = 53 000. Staining of T2 DNA was accomplished by incubating overnight T2 DNA ($1.6\times10^{-6}$ moles of bp/l) and acridine orange ($5.4\times10^{-6}$ M). This solution was then diluted 10-fold in 0.5× TBE containing 2% (v/v) β-ME. The final concentrations were: $1.6\times10^{-7}$ moles of bp/l T2 DNA, $5.4\times10^{-7}$ M AO, 2% (v/v) β-ME. Eight µl of this solution were used to prepare the microscope slides as previously described.

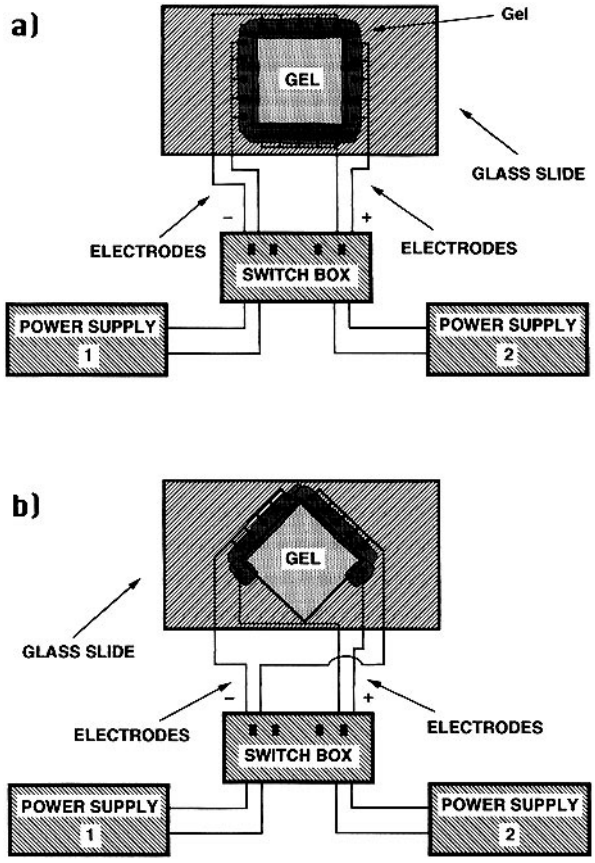


**Figure 2. (a)** Schematic drawing of a typical microscope slide used for experiments of 90° PFGE with 20 point electrodes arranged around a square contour to generate two orthogonal homogeneous and uniform electric fields. **(b)** Glass slide used for 120° PFGE experiments with 12 point electrodes arranged around a square contour to generate electric fields with angles between 90° and ~150°.

## Electrophoresis instrumentation

For 90° PFGE experiments a custom made microscope slide was equipped with 20 point electrodes arranged around a square contour, as shown in Figure 2a in a schematic diagram. This electrode geometry produces two uniform and homogeneous electric fields oriented at 90° with respect to one another. A switch-box connected to the 20 electrodes and to two different power supplies was used to switch the field between two orthogonal directions. A similar electrode configuration was used for 120° PFGE experiments where 12 point electrodes were employed, arranged as shown in Figure 2b. This electrode geometry produces two electric fields oriented at an angle of 90° at the top of the slide and ~150° near the bottom. This way, the reorientation behaviour of the DNA molecules could be studied at any arbitrary angle between 90° and 150° by simply observing DNA molecules in different positions of the slide. Also angles < 90° could be used by simply inverting the polarity of one of the electrode pairs.

**Table 1.** Properties of fluorescent dyes upon binding to dsDNA

| | Ethidium bromide | Acridine Orange | YOYO-1 |
|---|---|---|---|
| $\lambda^{ex}_{max}$ (nm) | 526 | 502 | 491 |
| $\varepsilon_{max}$ ($M^{-1}cm^{-1}$) | 3200 | 53000 | 99000 |
| $\lambda^{em}_{max}$ (nm) | 604 | 538 | 509 |
| Quantum yield ($\Phi$) | 0.15 | 0.43 | 0.52 |
| Fluorescence enhancement ($\psi$) | 21 | 1.5 | 460 |
| Binding affinity ($M^{-1}$) | $1.5 \times 10^5$ | $3.1 \times 10^4$ | $6 \times 10^8$ |
| Signal/background | 1.3 | 1.2 | 3.9 |

### Imaging instrumentation

An epi-illumination fluorescence microscope (Axiovert 35M, Zeiss) equipped with a 100× / 1.3 N.A. oil immersion Plan-Neofluar objective, and a high pressure Mercury lamp was used for all electrophoresis experiments. The microscope was coupled, through a high gain image intensifier (KS-1380 Videoscope International, LTD), to a high sensitivity video camera (VS2000N Videoscope International, LTD) designed specifically for critical low-light imaging. The DNA images presented here were recorded in real time using an 8 mm video camera recorder (CCD-V701, Sony Corporation). When acridine orange or YOYO-1 were used to fluorescently label the DNA a blue incident light filter set was employed (excitation filter BP 450–490, dichroic mirror FT 510, emission filter LP 520). In the case of ethidium bromide a green incident light filter set was used (excitation filter BP 510–560, dichroic mirror FT 580, emission filter LP 590). All observations were made immediately after preparing the glass slides and for no longer than 1 h. The molecules selected for study were all at least 5 microns distant from the glass/gel interface. The pictures were taken directly from a video screen by pausing the video-tape on a single frame. No image processing system was employed. Length measurements were performed directly from the screen, previously calibrated using a fluorescent grid of known dimensions. The photographs presented here are illustrations of the typical behavior encountered in a large number of observations.

In order to quantify signals from the DNA–dye complexes and the background, a charge-coupled device (CCD) camera (Star-1, Photometrics, Ltd) was used. This device made it possible to obtain linear signals over a dynamic range of ~4000. All instrumental parameters were kept constant to obtain accurate relative signals between samples and over time. Full CCD images were transferred to a MATROX image processor (Image-1/AT, Universal Imaging) for analysis.

## RESULTS AND DISCUSSION

### Improvement of signal/background using YOYO

In early attempts of imaging the dynamic behaviour of single DNA molecules by fluorescence microscopy it has been very difficult to obtain high-quality images using standard fluorescent dyes like ethidium bromide or acridine orange (19–21). In fact, the binding and spectroscopic characteristics of these dyes are such that relatively high DNA and dye concentrations must be employed, leading not only to confusion between different molecules, but also to a high and inhomogeneous fluorescence background. This drawback has clearly limited the application of this technique for the study of the physical properties and the dynamic behaviour of individual molecules of DNA under various experimental conditions.

In this context, our first goal was to understand the relationship between the DNA–dye complex and the corresponding image contrast, and, subsequently, to search for new fluorescent dyes that would improve the signal/background of the DNA images. Thus, we started out by characterizing the most important physical and spectral properties of several fluorescent dyes including the members of a new family of cyanine dyes recently designed and synthetized by Molecular Probes Inc. Some of these results are summarized in Table 1. In fact, the quality of fluorescence images of individual DNA molecules is controlled by those factors that determine the difference in fluorescence intensity between the molecules and the surrounding background. Clearly, the binding affinity of the dye for the DNA and the enhancement in the dye fluorescence upon binding to DNA are the critical factors determining the contrast, i.e. the intensity of the signal over the background. Instead, the extinction coefficient and the fluorescence quantum yield are the critical factors determining the overall brightness of a fluorescently labeled DNA molecule. Unfortunately, these conditions are poorly met by standard fluorescent dyes such as ethidium bromide or acridine orange (Table 1). On the other hand, it was found that a new dimeric cyanine dye, YOYO-1 (1,1′-(4,4,7,7-tetramethyl-4,7-diazaundecamethylene)-bis-4-[3-methyl-2,3-dihydro-(benzo-1,3-oxazole)-2-methyl-idene]-quinolinium tetraiodide), is characterized by a substantial increase in electrostatic binding affinity for DNA (due to the presence of four positive charges on the molecule) about three orders of magnitude higher than ethidium bromide and acridine orange (Table 1). The very high binding affinity of YOYO-1 for DNA greatly minimizes the amount of free dye in solution that, together with a high fluorescence enhancement upon binding to DNA (Table 1), leads to an extremely low fluorescence background (YOYO-1 is virtually non-fluorescent when free in water solution). Moreover, YOYO-1 bound to double-stranded DNA has 30-fold higher extinction coefficient and a 3-fold higher fluorescence quantum yield compared to ethidium bromide (Table 1). Therefore YOYO labeled DNA molecules result much brighter with a significantly lower background signal. Instead, acridine orange has, compared to ethidium bromide, lower binding constant and lower fluorescence enhancement upon binding, while it has a higher extinction coefficient and fluorescence quantum yield (Table 1). Therefore, DNA staining with acridine orange produces intrinsically brighter molecules than ethidium bromide (about as bright as YOYO-stained molecules) but with a lower contrast.

As will be seen later, the improvement in the quality of the images of individual DNA molecules stained with YOYO-1 is remarkable. The molecules appear much brighter in comparison

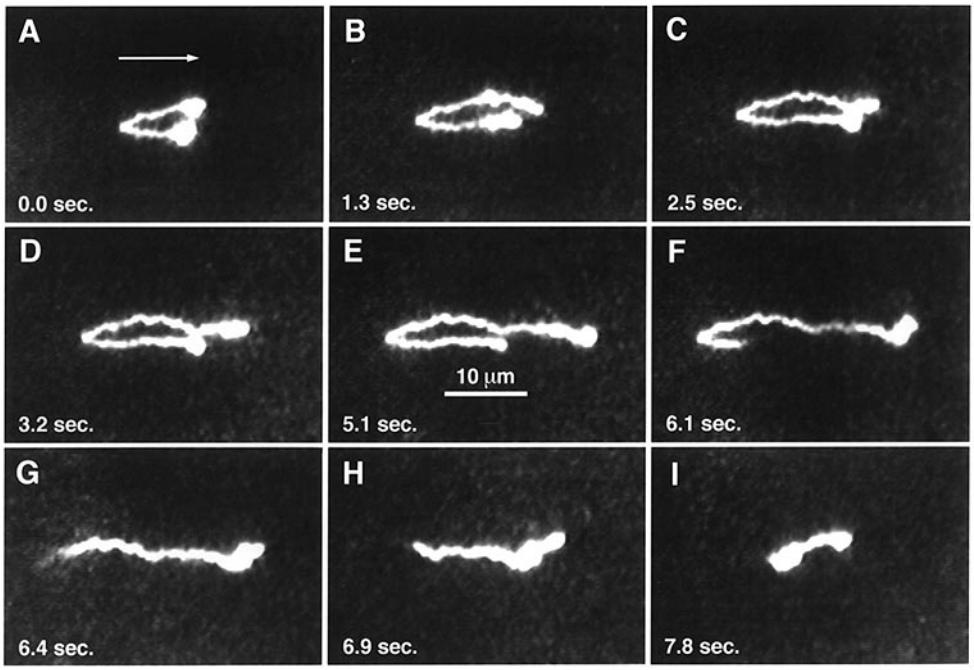


**Figure 3.** Time sequence of a T2 DNA molecule (164 kb) labeled with YOYO-1 and undergoing steady-field electrophoresis. The molecule is moving to the right in the direction of the arrow. DNA labeled with YOYO-1. Electric field, 8 V/cm.

with the standard staining of ethidium bromide or acridine orange and the background becomes very dark and more homogeneous. Moreover, the high affinity of YOYO-1 towards DNA made it possible to use very low DNA and dye concentration ($5 \times 10^{-9}$ moles of bp/l DNA, $1 \times 10^{-9}$ M YOYO-1) resulting in the presence of few bright molecules in the field of view of the microscope, increasing the contrast and avoiding confusion between molecules. Unfortunately, it turns out that under ordinary imaging conditions there is non-specific association between the dyes and background material (impurities in the solution or scratches and imperfections on the glass surface of both slide and coverslip). Also, this unspecific binding to non-target material is characterized by a significant fluorescence enhancement as well. This effect, together with the presence of several other sources of optical noise, result in a reduced signal/background compared to 'ideal' circumstances.

A minor drawback of the use of YOYO-1 to fluorescently label single DNA molecules is that the durability of real-time imaging experiments is limited because of the inevitable photosensitivity of the DNA–YOYO complex under high intensity illumination conditions (40). A similar extensive strand breaking had previously been observed to occur with acridine orange (41). Initially, only high concentrations (2–4%) of a free-radical scavenger like β-ME were used to reduce light-induced damage to the DNA molecules. However, also in the presence of β-ME the lifetime of YOYO-1-labeled DNA molecules was limited to only few seconds. Fortunately, since preliminary experiments had shown that this photosensitivity was mediated by molecular oxygen, the problem was overcome by carefully deoxygenating all the solutions and preparing the microscope slides under nitrogen atmosphere. Using such a 'trick', in combination with the use of β-ME, it was possible to extend the lifetime of the molecules to several minutes. DNA lifetime could be increased even further by using optical neutral density filters to reduce the excitation intensity. This clearly leads to a decrease of the overall brightness of the molecules, but allows optimal illumination conditions to be chosen depending on the application. Moreover, the depletion of molecular oxygen, well known to be a good quencher, also enhances the fluorescence quantum yield of YOYO-1, improving further the brightness of the DNA molecules.

## Molecular mechanisms of DNA motion during steady-field electrophoresis

Only recently fluorescence microscopy has been used to image individual DNA molecules undergoing agarose gel electrophoresis (19–26). As shown in Figure 3, under the application of a steady electric field the dynamics of the molecules turned out to be rather complex. The molecules migrate through the gel by a cyclic motion of alternating elongated and compact conformations, resembling the motion of a caterpillar. Elongated states form because the molecules remain hooked around gel fibers, extending both of the arms downfield, here named U-shapes (Fig. 3D), and then slipping off, with the longer arm driving the chain (Fig. 3F). The 'tail' then catches up with the 'head' and the molecule starts another caterpillar cycle (Fig. 3I). Increasing the electric field strength, the molecules become, on average, better aligned in the direction of the field and more elongated. However, the molecules never stretch totally to their theoretical contour length. This is due to the intrinsic entropic elasticity of the molecules and also to the zig-zag path through the agarose network that they are constrained to follow. The leading end is usually bunched up, appearing brighter than other parts of the molecule, since it has to find its way through the gel pores. On the other hand, the body of the DNA chain is usually stretched because the trailing end often remains wrapped around some gel fibers, and, since it is already threaded through pores, just follows along the same path of the

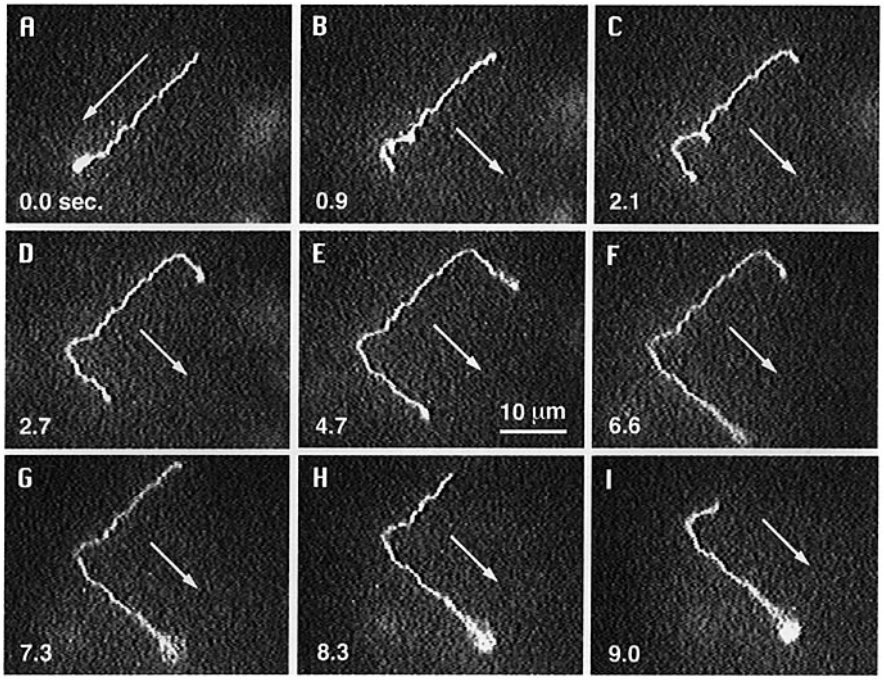


**Figure 4.** Sequence illustrating a T2 DNA molecule during 90° PFGE. The molecule is first moving to the lower left (**A**) in the direction of the arrow. Then the field is switched to the lower right (**B**). DNA stained with YOYO-1. Electric field, 10 V/cm. Clearly, under pulsed field conditions, the DNA molecules can be in any of the conformations shown in Figure 3 when the field is switched in direction either by 90° or by 120°. The sequences shown here and in Figure 6 start off with relatively elongated molecules so to better underline the difference in reorientation mechanism of 90° and 120° PFGE responsible for DNA separation.

'head'. Also, computer simulations (24,36–37) have clearly shown that in a caterpillar cycle, the head of the molecule moves at approximately constant speed. Thus, chain retardation is not controlled by the time required to form and slip out of the U-shapes, but by the sieving of the leading end through the gel pores. Since this process is clearly independent of molecular size it explains the failure of conventional electrophoresis for DNA molecules longer than 10–20 kb (1–2).

Here, the use of YOYO-1 has allowed a major improvement in the quality of the images. During electrophoresis, the DNA molecules labeled with ethidium bromide or acridine orange appear relatively bright under the microscope only if they are in a compact state. However, when the molecules assume elongated conformations they appear so dim that is barely possible to follow their contour, especially if part of them are out of the plane of focus. The quality of the images is also affected by the high and inhomogeneous background due to the molecules out of the plane of focus and to the presence of an excess of free dye in solution. On the contrary, DNA molecules labeled with YOYO-1 appear very bright, also in conditions of maximum extension (Fig. 3C–E), against a very dark and homogeneous background.

## Molecular mechanisms of separation in 90° PFGE and 120° PFGE

Fluorescence microscopy and computer simulations have shown that in DNA molecules undergoing 90° PFGE, the 'head' of the chain (that is bunched) usually remains the leading end of the molecule and turns the corners in the direction of the new field, entering new gel pores. Figure 4 shows a time sequence of a T2 DNA molecule reorienting by the leading end. Only a few short kinks (Fig. 4B–C) (where the molecule is doubled over on itself) are observed at the beginning of the reorientation, and these disappear very rapidly. Also, both ends of the molecule can extend and turn in the new direction (Fig. 4D–F) but eventually the leading end keeps driving the chain (Fig. 4G). This reorientation mechanism is also schematically shown in Figure 5A, where for simplicity the DNA molecule is drawn in a straight conformation. When the field is switched by an angle $\leq 90°$ the same end leads the molecule during the reorientation because the component of the new electric field along the previous path direction is either along the same direction the molecule was moving before the field was switched (for angles <90°) or it is zero (for angles = 90°). In this case, since the same end leads the molecule during the reorientation, the overall DNA motion is not very different from that observed during conventional (steady-field) electrophoresis (Fig. 3). Here, as well, chain retardation is controlled by the sieving of the leading end through the gel pores (a process independent of molecular size). Therefore, this reorientation mechanism provides a clear explanation for the poor separation obtained when angles $\leq 90°$ are employed in PFGE experiments. Only occasionally the 'tail' end of DNA molecules undergoing 90° PFGE was observed to turn in the direction of the field and sometimes even succeed in driving the chain.

On the other hand, in 120° PFGE, the DNA molecules usually reverse in their path, and what was the trailing end ('tail') during the previous pulse now becomes the 'head' and turns a corner in the direction of the new field. The former 'head' becomes the 'tail' and backtracks on its previous path. In Figure 6 is shown a time sequence of a T2 DNA molecule reorienting by the trailing end in 120° PFGE. This reorientation mechanism is also schematically shown in Figure 5B, where, again, the DNA molecule is drawn

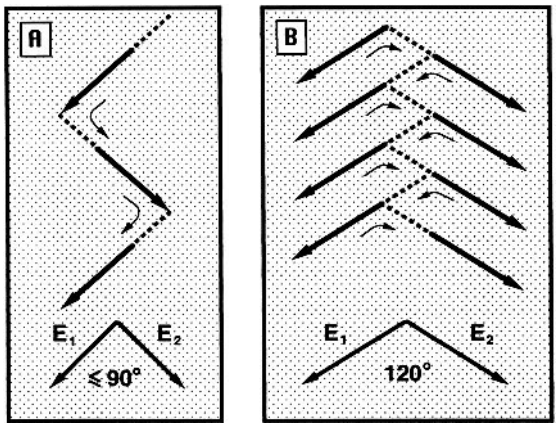


**Figure 5.** Schematic drawing of the different reorientation mechanisms in PFGE. When the electric field is switched by 90° the DNA molecule reorients by the leading end (**A**). When the field is switched by 120° the molecule reorients by the trailing end (**B**).

in a straight conformation for simplicity. When the field is switched by an angle of 120° (or any other angle ≥90°) the component of the new electric field along the previous orientation of the molecule is now in a direction opposite to the one along which the molecule was moving before and, therefore, the molecules are pulled back along their previous paths. Every time the electric field is switched in direction, all DNA molecules start their motion at the position of their 'tail', which clearly depends on the size and the elongation state of the molecules. Since, on average, longer molecules backtrack further than shorter ones, the net 'macroscopic' distance migrated clearly becomes size dependent, and this explains why a good size separation is achieved in 120° PFGE. The separation of a long and a short DNA molecule, reorienting according to this mechanism, is schematically shown in Figure 7.

Similar results were obtained during computer simulations based on a model that 'faithfully' reproduces the molecular mechanism of motion observed under the microscope (36–37). Figure 8 A and B shows a short (100 kb) and a long (300 kb) DNA molecule in a simulated 120° PFGE experiment. The longer molecule makes less progress because at the time when the electric field is switched in direction, its trailing end is further behind than the trailing end of the shorter molecule. Our simulations not only can reproduce the DNA dynamic motion observed under the fluorescence microscope, but also recover the characteristic mobility curves of real PFGE experiments (24,36).

The results of our experiments are in good qualitative agreement with a mechanism originally suggested by Southern *et al.* (27) whose main idea turned out to be basically correct. However, this model is based on the wrong assumption that the DNA molecule is considered as moving in a straight conformation through the gel while DNA elasticity and U-shape formation (not known at the time the model was developed) are not considered. In fact, because of this limitation, Southern's model fails in explaining the success of FIGE (Field-Inversion Gel Electrophoresis) methods (10). Also, our observations are in perfect agreement with the outcome of macroscopic electrophoresis experiments of long DNA chromosomes under 90° and 120° PFGE conditions (42–43).

On the other hand, our experimental results allow the conclusion that the original idea for size separation (29) described in Figure 1 is basically wrong because DNA molecules are instead primarily separated by means of the different mechanism described above. In fact, the major limitation of that model is that it does not consider that the DNA molecules continue migrating through the gel also during the reorientation process. Therefore, even if it is true that molecular reorientation time slightly

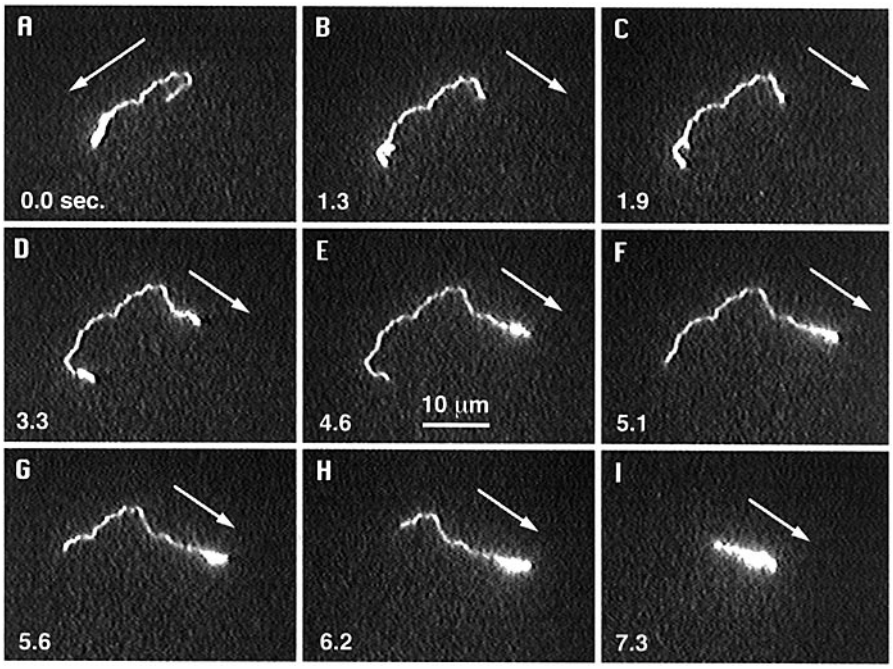


**Figure 6.** Time sequence of a T2 DNA molecule undergoing 120° PFGE. The molecule is first moving to the lower left (**A**). Then the field is switched to the lower right (**B**). Notice that the 'tail' end of the molecule drives the chain during the reorientation process. DNA labeled with YOYO-1. Electric field, 8 V/cm.

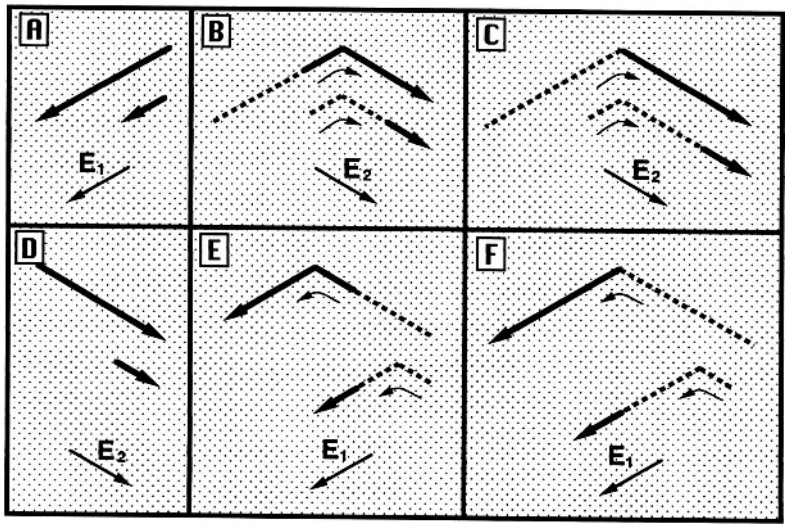


**Figure 7.** Schematic drawing of the separation mechanism during 120° PFGE. Longer molecules are separated from shorter ones because at each reorientation they backtrack in the gel of a longer distance proportional to their size therefore remaining behind.

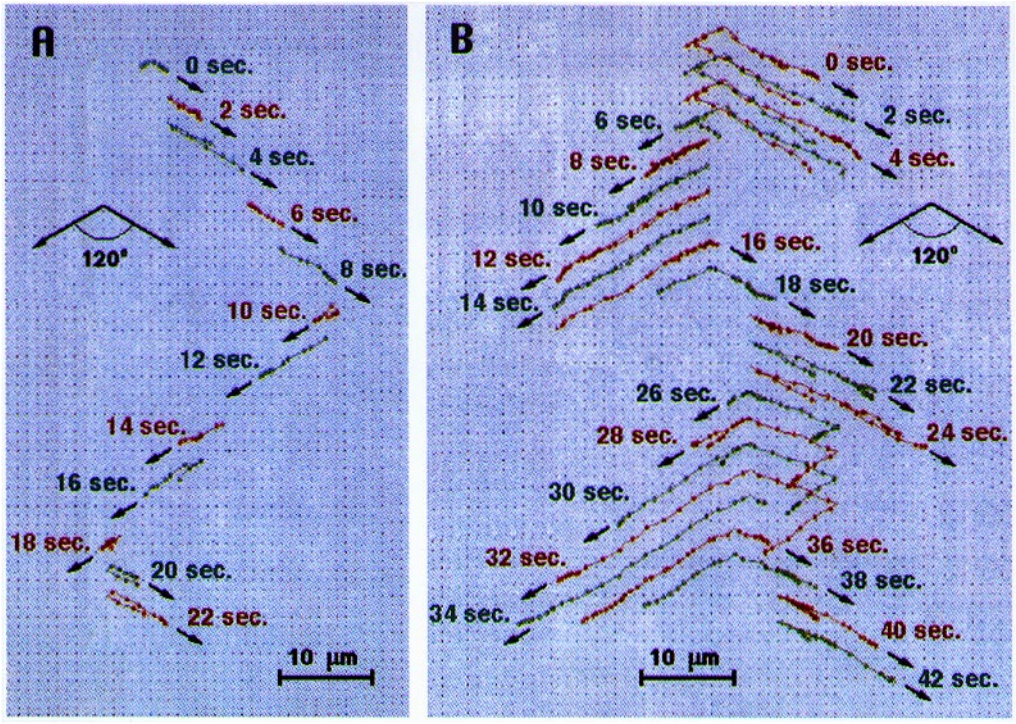


**Figure 8.** Computer simulation of (**A**) a short DNA molecule (100 kb) and (**B**) a long DNA molecule (300 kb) undergoing 120° PFGE. The field pulls the molecules alternatively towards the lower right and left in the direction of the arrows. Successive molecular conformations, 2 s apart, are colored differently and shifted downward for clarity. Electric field, 6 V/cm; pulse time, 10 s.

increases with DNA size, the 'heads' of molecules of different lengths travel almost the same distance during the reorientation process. A variety of shapes contribute to slightly retard the reorientation of larger molecules and, therefore, slightly improve size separation in PFGE: (i) narrow based U-shapes (Fig. 6A) such as those occurring in steady-field electrophoresis (Fig. 3C); (ii) broad based U-shapes where both ends extend downfield from the elastic chain (Fig. 6B–E); and (iii) kinks sometimes form in the middle of the molecule (Fig. 6B–C). Similar shapes were also observed for computer simulated DNA molecules as shown in Figure 8B.

A major step for a clear understanding of the mechanisms of motion and reorientation of DNA molecules during pulsed field electrophoresis has been accomplished. This should provide the basis for the rational optimization of these techniques. Such understanding should eventually lead to new separation protocols

which require reduced running times, give improved resolution and eventually may even separate larger DNA molecules than presently possible (18).

## REFERENCES


1 McDonell,M.W., Simon,M.N. and Studier,F.W. (1977) *J. Mol. Biol.*, **110**, 119–146.
2 Fangman,W.L. (1978) *Nucleic Acids Res.*, **5**, 653–665.
3 Hervet,H. and Bean,C.P. (1987) *Biopolymers*, **26**, 727–742.
4 Stellwagen,N.C. (1985) *Biopolymers*, **24**, 2243–2255.
5 Schwartz,D.C. and Cantor,C.R. (1984) *Cell*, **37**, 67–75.
6 Carle,G.F. and Olson,M.V. (1984) *Nucleic Acids Res.*, **12**, 5647–5664.
7 Chu,G., Vollrath,D. and Davis,R.W. (1986) *Science*, **234**, 1582–1585.
8 Vollrath,D. and Davis,R.W. (1987) *Nucleic Acids Res.*, **15**, 7865–7876.
9 Anand,R. (1986) *Trends Genet.*, **2**, 278–283.
10 Carle,G.F., Frank,M. and Olson,M.V. (1986) *Science*, **232**, 65–68.
11 Serwer,P. (1987) *Electrophoresis*, **8**, 301–304.
12 Gardiner,K. and Patterson,D. (1988) *Nature*, **331**, 371–372.
13 Bancroft,I. and Wolk,C.P. (1988) *Nucleic Acids Res.*, **16**, 7405–7418.
14 Lai,E., Birren,B.W., Clark,S.M., Simon,M.L. and Hood,L. (1989) *BioTechniques*, **7**, 34–42.
15 Olson,M.V. (1989) In Setlow,J.K. (ed.) *Genetic Engineering.* Plenum Publishing Corporation, New York, Vol. 11, pp. 183–237.
16 Chu,G. (1990) *Methods*, **1**, 129–142.
17 Gardiner,K. (1991) *Anal. Chem.*, **63**, 658–665.
18 Orbach,M.J., Vollrath,D., Davis,R.W. and Yanofsky,C. (1988) *Mol. Cell. Biol.*, **8**, 1469–1473.
19 Smith,S.B., Aldridge,P.K. and Callis,J.B. (1989) *Science*, **243**, 203–206.
20 Schwartz,D.C. and Koval,M. (1989) *Nature*, **338**, 520–522.
21 Gurrieri,S., Rizzarelli,E., Beach,D. and Bustamante,C. (1990) *Biochemistry*, **29**, 3396–3401.
22 Bustamante,C., Gurrieri,S. and Smith,S.B. (1990) *Methods*, **1**, 151–159.
23 Rampino,N.J. (1991) *Biopolymers*, **31**, 1009–1016.
24 Bustamante,C., Gurrieri,S. and Smith,S.B. (1993) *Trends Biotech.*, **11**, 23–30.
25 Oana, H, Masubuchi,Y., Matsumoto,M., Doi,M., Matsukawa,Y. and Yoshikawa,K. (1994) *Macromolecules*, **27**, 6061–6067.
26 Larsson,A. and Akerman,B. (1995) *Macromolecules*, **28**, 4441–4454.
27 Southern,E.M., Anand,R., Brown,W.R.A. and Fletcher,D.S. (1987) *Nucleic Acids Res.*, **15**, 5925–5943.
28 Deutsch,J.M. (1987) *Phys. Rev. Lett.*, **59**, 1255–1258.
29 Cantor,C.R., Smith,C.L. and Mathew,M.K. (1988) In Engelman,D.M, Cantor,C.R. and Pollard,T.D. (eds) *Annual Reviews of Biophysics and Biophysical Chemistry.* Annual Reviews, Inc., Palo Alto, CA, Vol. 17, pp. 287–304.
30 Rye,H.S., Yue,S., Wemmer,D.E., Quesada,M.A., Haugland,R.P., Mathies,R.A, Glazer,A.N. (1992) *Nucleic Acids Res.*, **20**, 2803–2812.
31 Glazer,A.N. and Rye,H.S. (1992) *Nature*, **359**, 859–861.
32 Rye,H.S., Yue,S., Quesada,M.A., Haugland,R.P., Mathies,R.A, Glazer,A.N. (1993) In Wu,R. (ed.) *Methods Enzymol.*, **217**, 414–431.
33 Larsson,A., Carlsson,C., Jonsson,M. and Albinsson,N. (1994) *J. Am. Chem. Soc.*, **116**, 8459–8465.
34 Netzel,T.L., Nafisi,K., Zhao,M.,Lehnard,J.R. and Johnson,I. (1995) *J. Phys. Chem.*, **99**, 17936–17947.
35 Carlsson,C., Larsson,A. and Jonsson,M. (1996) *Electrophoresis*, **17**, 642–651.
36 Smith,S.B., HellerC. and Bustamante,C. (1990) *Biochemistry*, **30**, 5264–5274.
37 Smith,S.B., Gurrieri,S., Bustamante,C. (1990) In Lai.E. and Birren,B.W. (eds) *Current Communications in Cell and Molecular Biology. Electrophoresis of Large DNA Molecules: Theory and Applications.* Cold Spring Harbor Press, Cold Spring Harbor, New York, Vol. 1, pp. 55–79.
38 Weber,G. and Teale,F.W.G. (1957) *Trans. Farad. Soc.*, **53**, 646–655.
39 Haughland,R.P. (1992) In Larison,K.O. (ed.) *Fluorescent Probes and Research Chemicals.* Molecular Probes, Inc., Eugene, OR, pp. 224.
40 Akerman,B. and Tuite,E. (1996) *Nucleic Acids Res.*, **24**, 1080–1090
41 Freifelder,D. Davison,P.F. and Geiduschek,E.P. (1961) *Biophys. J.*, **1**, 389–400.
42 Hutson,M.S., Holzwarth,G., Duke,T. and Viovy,J.L. (1995) *Biopolymers*, **35**, 297–306.
43 Neitzey,L.M., Holzwarth,G., Duke,T. and Viovy,J.L. (1995) *Biopolymers*, **35**, 307–317.